Dislocation-vibration model for nonclassical rotational inertia

Izumi Iwasa*
Fuji Xerox Company, Ltd., Nakai-machi, Kanagawa 259-0157, Japan
(Received 7 March 2010; published 29 March 2010)

A dislocation model for the nonclassical rotational inertia is proposed. Temperature dependence of the period of the torsional oscillator containing solid helium is derived from the variation in the average pinning length of dislocations in solid helium. The mechanism is that the vibration of dislocations causes the wave number of the shear wave in solid helium to increase. Consequently the apparent moment of inertia of solid helium is increased with increasing temperature.

DOI: 10.1103/PhysRevB.81.104527 PACS number(s): 67.80.−s, 61.72.Hh, 62.40.+i, 67.90.+z

I. INTRODUCTION

Since the first observation of nonclassical rotational inertia (NCRI) of solid helium,[1,2] several groups have confirmed the existence of the effect.[3–6] However, the origin of NCRI is not clear yet.[7] The decrease in the period of the torsional oscillator (TO) at low temperatures seemed to indicate that a part of the mass of solid helium was decoupled from the torsional oscillation. The concept of supersolid was proposed as a possible mechanism for NCRI and the NCRI fraction (NCRIF) was obtained. The NCRIF was decreased when the rim velocity was above about 10 μm/s, which was interpreted to be the supersolid critical velocity. The size of NCRIF varied in a wide range from 0.03% to 20% but its onset temperature was rather reproducible as far as commercially available pure ^{4}He gas containing about 300 ppb ^{3}He was used. NCRI was observed both in cylindrical and annulus TOs. The highest NCRIF of 20% was reported for rapidly cooled solid helium in an annulus TO.[8] The decrease in NCRIF by annealing,[3] the increase in the onset temperature with the ^{3}He concentration,[9] and the hysteresis with respect to the rim velocity[4] and to the temperature[10] indicate that the observed NCRI is not an intrinsic property of solid helium, but an effect of defects such as dislocations, grain boundaries, and ^{3}He impurities in solid ^{4}He.

Most of the ^{4}He crystals studied in the TO experiments were grown with the blocked capillary method.[9] They were probably polycrystalline and contained both grain boundaries and dislocations. However, Clark *et al.*[11] have grown high-quality crystals in their TO with the open capillary method and still observed NCRI in all the samples. They have excluded the grain-boundary model[12] and suggested dislocations as possible defects responsible for NCRI.

The existence of dislocations in solid helium was first pointed out in the plastic deformation experiments.[13,14] Then ultrasonic studies revealed the unique properties of the dislocations in hcp ^{4}He crystals.[15,16] Namely, the basal dislocations whose slip plane was the basal plane of the hexagonal crystal could oscillate resonantly with the sound wave in the megahertz region at temperatures below 1 K, thereby inducing the sound velocity change and sound attenuation. The same phenomena were also observed in hcp ^{3}He crystals.[17] On the other hand, the ultrasonic properties of the dislocations in bcc ^{3}He crystals[17,18] were found to be very different from those in hcp ^{4}He and hcp ^{3}He crystals as a result of the Peierls potential.

Day and Beamish[19] have found that the shear modulus μ of hcp ^{4}He at low frequencies was increased by about 10% as the temperature was lowered from 200 to 18 mK. They explained the variation in μ in terms of dislocations pinned by ^{3}He atoms. There were several similarities between μ and TO measurements. However, it was believed[7,19] that an increase in μ would intensify the coupling of solid helium to the TO and increase its period. The observed period was decreased at low temperatures instead. In the following we will seek a theoretical relationship between the dislocation motion in solid helium and the period of TO.

II. MODEL

A. Torsional oscillator

The rotational equation of motion for a TO containing solid helium is given by

$$I_{\mathrm{TO}}\frac{d^2\phi}{dt^2} = -\kappa\phi + \tau, \tag{1}$$

where I_{TO} is the moment of inertia of the TO, ϕ is the torsional angle, κ is the torsional spring constant, and τ is the torque exerted by solid helium on the wall of the TO. We employ a cylindrical coordinate system (r,θ,z) with the z axis coinciding with the axis of the cylinder and assume the displacement occurs only in the θ direction, namely, $u_\theta = u_\theta(r,t)$. As the surface of solid helium moves together with the TO, the boundary condition at the cylindrical wall is

$$u_\theta(R,t) = u_0 e^{-i\omega t}, \tag{2}$$

where u_0 is the amplitude of the rim displacement of the TO and ω is the angular frequency. We note that $\phi = u_\theta(R,t)/R$.

The oscillation of the TO induces periodical stress, $\sigma(r)$, in solid helium. As a reaction solid helium exerts a force on the wall of the TO. We consider a cylindrical TO with radius R and height H and assume for simplicity that the cylinder is sufficiently long so that the effect of the top and bottom plates can be neglected. Then the torque is obtained to be

$$\tau = -2\pi R^2 H\sigma(R). \tag{3}$$

The assumption above may not be good for actual cylindrical geometry but good enough for annulus geometry.

Using the theory of elasticity,[20] the displacement is obtained analytically as

$$u_\theta(r,t) = u_0 \frac{J_1(k_r r)}{J_1(k_r R)} e^{-i\omega t}, \tag{4}$$

where J_1 denotes Bessel's function of order 1 and k_r is the wave number for shear wave in the radial direction which satisfies the dispersion relation

$$\mu k_r^2 = \rho\omega^2. \tag{5}$$

μ and ρ are the shear modulus and the density of solid helium, respectively. The shear stress, $\sigma_{r\theta}$, can be calculated from the displacement to be

$$\sigma_{r\theta} = -\mu u_0 k_r \frac{J_2(k_r r)}{J_1(k_r R)} e^{-i\omega t}, \tag{6}$$

where J_2 denotes Bessel's function of order 2. $k_r R$ is smaller than unity for a typical TO ($u_0=1$ nm, $k_r=0.02$ mm^{-1}, $R=4$ mm, and $\omega/2\pi=1000$ Hz), so that J_1 and J_2 can be expanded in power series of $k_r r$.

In the first-order approximation the stress becomes

$$\sigma_{r\theta} = -\frac{\mu k_r^2 r^2}{4}\phi = -\frac{\rho\omega^2 r^2}{4}\phi. \tag{7}$$

By using the moment of inertia of solid helium $I_{\mathrm{He}} = \frac{\pi}{2} R^4 H \rho$, the torque becomes

$$\tau = I_{\mathrm{He}}\omega^2\phi. \tag{8}$$

Then Eq. (1) becomes equivalent to the torsional equation of motion with a total moment of inertia $I_{\mathrm{TO}}+I_{\mathrm{He}}$ and the period is independent of the shear modulus;

$$p = \frac{2\pi}{\omega} = 2\pi\sqrt{\frac{I_{\mathrm{TO}}+I_{\mathrm{He}}}{\kappa}}. \tag{9}$$

The second-order approximation has been derived by Clark *et al.*;[10]

$$p = 2\pi\sqrt{\frac{I_{\mathrm{TO}} + I_{\mathrm{He}}\left(1+\frac{\rho\omega^2 R^2}{24\mu}\right)}{\kappa}}. \tag{10}$$

As the temperature is lowered, μ is increased[19] and then p is decreased according to Eq. (10). This is qualitatively in accordance with experimental results, but quantitatively, the change in p is too small.

B. Effect of dislocations

The effect of dislocations on the period of the TO is analyzed in the following. A dislocation is a linear lattice defect which is characterized by the direction vector l and Burgers vector b. Dislocation lines form a three-dimensional network as shown in Fig. 1(a). Dislocation lines terminate at the interface wall with the termination being a strong pinning point. Dislocation lines are also strongly pinned at the nodes of the network. These strong pinning points are characterized by their nonconservative motion.[21] L_N is the average network pinning length, which is assumed to be constant throughout a series of experiment except for the case when the sample is annealed. A typical value of L_N is a few micrometer from the ultrasonic measurements.[16] Dislocation lines are weakly pinned by ^{3}He impurity atoms. L_i is the average impurity pinning length, which depends on the temperature T and the bulk ^{3}He concentration x_3,

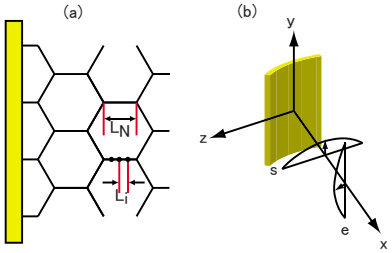

FIG. 1. (Color online) (a) Schematic dislocation network in solid helium. L_N: network pinning length, L_i: impurity pinning length. (b) Local coordinate system with two dislocations which glide on yz plane. s: screw dislocation, e: edge dislocation. The small arrows indicate the direction of dislocation motion.

$$L_i = g x_3^{-2/3} e^{-2W_0/3T}, \tag{11}$$

where $g=3.4\times10^{-9}$ m is a constant and $W_0=0.3$ K is the binding energy.[22] The factor $-2/3$ arises from the condition that L_i is proportional to $c^{-2/3}$, where

$$c = x_3 e^{W_0/T} \tag{12}$$

is the local concentration of ^{3}He near the dislocation line. The average length of dislocation segments L approaches L_N at high temperatures and L_i at low temperatures. The transition temperature from L_N to L_i depends on x_3. As the number of impurity pinning points is Λ/L_i and that of network pinning points is Λ/L_N, an interpolation of L_N and L_i is given by

$$L = \frac{\Lambda}{\frac{\Lambda}{L_i}+\frac{\Lambda}{L_N}} = \frac{L_N L_i}{L_N + L_i}. \tag{13}$$

L_N, L_i, and L at different x_3 are shown in Fig. 2(a).

The glide plane of a dislocation is defined as a lattice plane containing both l and b. We introduce a local coordinate system the origin of which is a point on the cylindrical wall of the TO as depicted in Fig. 1(b). x is the direction from the cylindrical wall to the rotational axis of the TO, y is parallel to the rotational axis and z is the tangential direction of the cylinder. As the TO oscillates, a shear wave propagating in x direction is excited in solid helium which causes displacement in z direction. The shear stress in solid helium excited by the torsional oscillation is given by

$$\sigma(x,t) = \sigma_0 e^{i(k'x-\omega t)}, \tag{14}$$

where k' is the wave number of the shear wave under the existence of dislocations. Two types of dislocations whose glide plane is the yz plane can interact with the shear stress Eq. (14): one is the screw dislocation with $b\|z$ and $l\|z$, the other is the edge dislocation with $b\|z$ and $l\|y$ as shown in Fig. 1(b). When the shear stress is applied, the screw dislocation moves in y direction and the edge dislocation moves in z direction. Ultrasonic experiments indicate that movable dislocations in hcp ^{4}He are basal edge dislocations. Hence

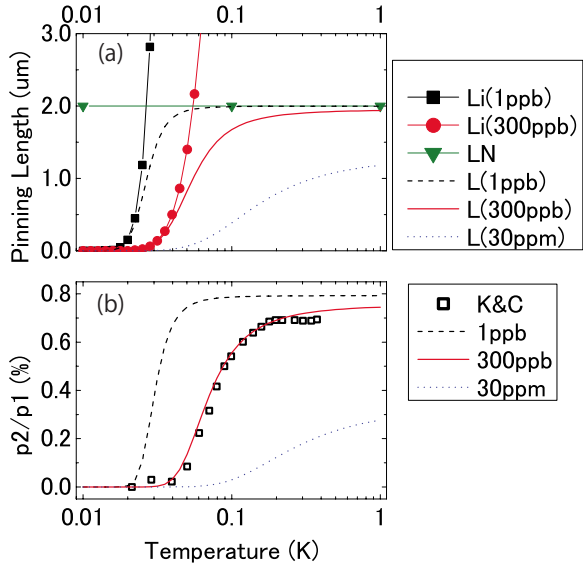

FIG. 2. (Color online) (a) Temperature dependences of L_N, L_i, and L with $L_N=2.0\times10^{-6}$ m. (b) Temperature dependences of p_2/p_1 at $x_3=1$ ppb, 300 ppb, and 30 ppm calculated from Eqs. (13) and (29), with $\Omega\Lambda=1.78\times10^{10}$ m^{-2}, $L_N=2.0\times10^{-6}$ m, $\nu=0.3$, and the experimental data of NCRI (Ref. 23) converted to p_2/p_1.

we assume the dislocations to be the edge dislocation $b\|z$, $l\|y$ in the following.

According to Granato and Lücke,[24] the strain of a crystal containing dislocations is a sum of the elastic part and the dislocation part,

$$\epsilon=\epsilon_{\rm el}+\epsilon_{\rm dis}. \tag{15}$$

The elastic part is related to the stress as

$$\epsilon_{\rm el}=\frac{\sigma}{\mu_{\rm el}}, \tag{16}$$

where $\mu_{\rm el}$ is the elastic shear modulus without the effect of dislocations. The resonance frequency of a dislocation segment of length L is given by

$$\omega_0=\frac{1}{L}\sqrt{\frac{2\mu_{\rm el}}{(1-\nu)\rho}}, \tag{17}$$

where ν is Poisson's ratio. A typical value is $\omega_0/2\pi=16$ MHz for $L=5$ μm. Assuming $\omega\ll\omega_0$ and that the damping constant for dislocation motion $B=B_0T^3$ is negligible at $T<1$ K, we obtain the dislocation part of the strain to be

$$\epsilon_{\rm dis}=\frac{\Omega\Lambda\sigma}{\pi\rho\omega_0^2}, \tag{18}$$

where Ω is an orientation factor depending on the polarization of the elastic wave and the crystal orientation, and Λ is the dislocation density. A typical value of $\Omega\Lambda$ is 10^8-10^9 m^{-2} in the longitudinal ultrasonic measurements.[16] The equation of motion of solid helium containing dislocations is given by

$$\rho\frac{\partial^2\epsilon}{\partial t^2}=\frac{\partial^2\sigma}{\partial x^2}. \tag{19}$$

From Eqs. (14)–(19) we are led to

$$\mu_{\rm el}k'^2=\rho\omega^2\left(1+\frac{\mu_{\rm el}\Omega\Lambda}{\pi\rho\omega_0^2}\right). \tag{20}$$

This is the dispersion relation of solid helium with dislocations which should be used instead of Eq. (5).

Corresponding to Eq. (15) the displacement consists of the elastic part and the dislocation part,

$$u=u_{\rm el}+u_{\rm dis}. \tag{21}$$

Because the dislocations are pinned at the interface wall, the dislocation part of the displacement is negligible at the boundary. Hence the boundary condition of the TO is given by

$$u_{\rm el}(R,t)=u_0e^{-i\omega t}. \tag{22}$$

The elastic displacement and the stress in the solid helium become

$$u_{\rm el}(r,t)=u_0\frac{J_1(k'r)}{J_1(k'R)}e^{-i\omega t} \tag{23}$$

and

$$\sigma(r)=-\frac{\mu_{\rm el}k'^2r^2}{4}\phi=-\frac{\rho\omega^2r^2}{4}\left(1+\frac{\mu_{\rm el}\Omega\Lambda}{\pi\rho\omega_0^2}\right)\phi, \tag{24}$$

instead of Eqs. (4) and (7), respectively. Then the torque is given by

$$\tau=I_{\rm He}\omega^2\left(1+\frac{\mu_{\rm el}\Omega\Lambda}{\pi\rho\omega_0^2}\right)\phi, \tag{25}$$

and finally we obtain the period to be

$$p=2\pi\sqrt{\frac{I_{\rm TO}+I_{\rm He}\left(1+\frac{\mu_{\rm el}\Omega\Lambda}{\pi\rho\omega_0^2}\right)}{\kappa}}. \tag{26}$$

In the case of an annulus TO, the derivation is more tedious but the final results are the same as Eqs. (25) and (26) with a replacement for the moment of inertia

$$I_{\rm He}=\frac{\pi}{2}(R_0^2+R_1^2)(R_0^2-R_1^2)H\rho, \tag{27}$$

where R_0 and R_1 are the outer and inner radius of the annulus, respectively.

III. ANALYSIS

To compare with experiments Eq. (26) is rewritten to

$$p=p_0+p_1+p_2, \tag{28}$$

where $p_0=2\pi\sqrt{I_{\rm TO}/\kappa}$ is the period of the empty TO, $p_1=(I_{\rm He}/2I_{\rm TO})p_0$ is the change in the period due to loading with solid helium, and p_2 is the dislocation contribution to the period change,

$$p_2 = \frac{\mu_{\rm el}\Omega\Lambda}{\pi\rho\omega_0^2} p_1 = \frac{\Omega\Lambda L^2(1-\nu)}{2\pi} p_1. \tag{29}$$

Figure 2(b) shows the temperature dependences of p_2/p_1 at $x_3=1$ ppb, 300 ppb and 30 ppm calculated from Eq. (29) and an experimental data of NCRI (Ref. 23) at $x_3=300$ ppb converted to p_2/p_1. Parameters for L_i are taken from the ultrasonic measurements. Fit parameters are $L_N=2.0\times10^{-6}$ m and $\Omega\Lambda=1.78\times10^{10}$ m^{-2}, which are consistent with the ultrasonic dislocation parameters.

In the present model the TO period representing the intrinsic moment of inertia of solid helium is p_0+p_1 measured at low temperatures, where ^{3}He atoms completely pin the dislocations. As the temperature increases the average pinning length L becomes longer and the dislocation contribution p_2 is increased. The effect of dislocation vibration is to increase the wave number of the shear wave. As a result, the stress amplitude in solid helium induced by the torsional oscillation is increased, which in turn increases the torque on the TO, and consequently the period of the TO is increased. In other words the apparent moment of inertia of solid helium is increased.

IV. DISCUSSION

Day and Beamish[19] measured the strain and stress to derive the shear modulus. The strain they measured is the total strain appearing in the left-hand side of Eq. (15). Therefore what they have obtained is the macroscopic shear modulus

$$\mu_m = \frac{\sigma}{\epsilon} = \frac{\sigma}{\epsilon_{\rm el}+\epsilon_{\rm dis}}. \tag{30}$$

Using Eqs. (16)–(18), we obtain

$$\mu_m = \frac{\mu_{\rm el}}{1+\dfrac{\mu_{\rm el}\Omega\Lambda}{\pi\rho\omega_0^2}} \approx \mu_{\rm el}\left[1-\frac{\Omega\Lambda L^2(1-\nu)}{2\pi}\right]. \tag{31}$$

Equation (31) describes that the temperature dependence of the macroscopic shear modulus is also caused by the temperature dependence of L as Day and Beamish explained.

^{3}He atoms are weak pinning points. The force on a pinning point is approximately given by $f=L_i a\sigma$. When f exceeds a critical value f_c, the dislocation breaks away from the pinning point. As the stress amplitude increases, more dislocation segments break away from ^{3}He atoms and L becomes longer. As a result, the period of TO is increased. Therefore the observed amplitude dependence of the period is a consequence of the amplitude dependence of the pinning length.

Likewise the observed hysteresis of the period is a consequence of the hysteresis of the pinning length. At low stress level and at low T, the average pinning length L is equal to L_i. As the stress (or T) is increased L stays equal to L_i until the stress amplitude reaches a critical value. At higher stress level (or higher T) dislocations break away from ^{3}He atoms and L becomes longer. When the stress (or T) is decreased L remains long because the dislocations are oscillating. Moving dislocations are not readily pinned because it takes time for ^{3}He atoms to arrive at a dislocation line.[22] This hysteresis of L leads to the hysteresis of the period of TO.

It has been theoretically predicted that the core of a perfect screw dislocation parallel to the c axis becomes superfluid.[25] However, the screw dislocation has a large Burgers vector $b=\sqrt{8/3}a$ so that it tends to relax to configurations with lower energy[26] because the dislocation energy per unit length is approximately proportional to b^2. Hence the number of perfect screw dislocations must be much smaller than that of other dislocations. It is unlikely that a network of perfect screw dislocations exists in solid helium, which supports superflow throughout the sample. On the other hand, dislocations in hcp ^{4}He with the smallest Burgers vector are partial dislocations in the basal plane with $b=\sqrt{1/3}a$. They are calculated to be insulating.[27]

One of the experimental results which is considered to be an evidence for the supersolid model is the disappearance of NCRI in the cells with blocked annulus.[2,28] However, the present dislocation model can explain the disappearance as a difference of stress fields in blocked and unblocked annulus cells. In an unblocked cell, there exists only a circular shear stress field $\sigma_{r\theta}$. The barrier in a blocked cell, on the other hand, generates a compressive stress field $\sigma_{\theta\theta}$ in solid helium which causes two effects. Firstly, $\sigma_{\theta\theta}$ removes a part of the torque in Eq. (1) from $\sigma_{r\theta}$. Secondly, $\sigma_{\theta\theta}$ suppresses the amplitude of dislocation vibration severely. Consequently, p_2 becomes smaller. A TO experiment with a partially blocked annulus, i.e., the upper half blocked at one place and the lower half blocked at another place, would distinguish between the supersolid and dislocation mechanisms. The partial barriers cannot stop superflow but they can suppress the dislocation vibration as much as a perfect barrier.

The TO period change is always accompanied by a dissipation peak. In the present dislocation model, the dissipation is ascribed to damping of the dislocation vibration in solid helium and given by[24]

$$Q^{-1} = 2\Delta_a \frac{\omega d}{(\omega_0^2-\omega^2)^2+\omega^2 d^2}, \tag{32}$$

where $\Delta_a=(8\Omega\Lambda\mu)/(\pi^2\rho)$ is a constant independent of temperature and d is the temperature-dependent damping constant for dislocation motion. Note that ω_0 depends on temperature from Eqs. (11), (13), and (17),

$$\omega_0 = \left(\frac{x_3^{2/3}e^{2W_0/3T}}{g}+\frac{1}{L_N}\right)\sqrt{\frac{2\mu_{\rm el}}{(1-\nu)\rho}}. \tag{33}$$

The contribution of thermal phonons to d is negligible at temperatures below 1 K.[16] The origin of dislocation damping is the interaction of dislocation motion with the atmosphere of ^{3}He atoms formed around the dislocation line, whose concentration is given by Eq. (12). If we assume the damping constant to be proportional to $c^{2/3}$ similar to $1/L_i$, then Eq. (32) can be fitted to the experimental dissipation peak as shown in Fig. 3. The damping constant is determined to be

$$d = 2.58\times10^8 e^{0.2/T}\ {\rm s}^{-1}. \tag{34}$$

Relaxation models of glass,[29] superglass,[30] and viscoelasticity[31] can account for the dissipation peak to some extent. The advantage of these models is that they can de-

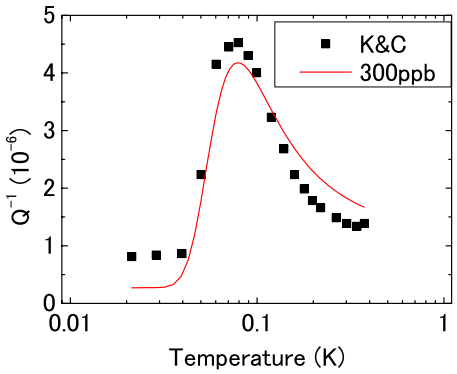

FIG. 3. (Color online) Dissipation data (Ref. 23) and calculation from Eqs. (32) and (34). Values of $\Omega\Lambda$ and L_N are taken to be the same as those in Fig. 2(b).

scribe the dissipation peak and the change in TO period simultaneously. Quantitative fitting of the dissipation and period with a single relaxation time, however, is not satisfactory.[29–31] The present dislocation model differs from those relaxation models in that not only the relaxation time, which is given by d/ω_N^2, but also the frequency of the vibrational modes, ω_0, depends on temperature. Here ω_N is the resonance frequency corresponding to L_N.

The present model is based on the unique property of solid helium that basal dislocations in the hcp ^{4}He crystal are movable on the basal plane. The crystal structure is crucial while the quantum statistics of atoms is not important. Hence one expects similar NCRI and similar change in μ to occur in hcp ^{3}He while no such phenomena in bcc ^{3}He. Recently West *et al.*[32] have measured the period of a TO and the shear modulus in ^{3}He crystals with bcc and hcp structures. In the case of bcc ^{3}He, no drop in the TO period and no increase in μ were observed in agreement with the present model. In the case of hcp ^{3}He, an increase in μ was observed in agreement with the model, but no drop in the TO period was observed. The final observation is inconsistent with the present model except for a special case that the orientation factor is null. Such a case is possible when the c axis of the helium crystal is parallel to the rotational axis. As the NCRI data presented in the Ref. 32 is limited to only one sample for hcp ^{3}He, more study is desirable especially at higher pressures.

V. CONCLUSION

In conclusion, the so-called nonclassical rotational inertia is caused by the variation in the average pinning length of dislocations in solid helium. The period change in TO and the variation in the shear modulus are explained in the same framework.

ACKNOWLEDGMENTS

The author is indebted to S. Ishioka for providing the analytical solution of elasticity in the cylindrical geometry. He also acknowledges stimulating discussions with M. Kubota.

*iwasa.izumi@fujixerox.co.jp

[1] E. Kim and M. H. W. Chan, Nature (London) **427**, 225 (2004).
[2] E. Kim and M. H. W. Chan, Science **305**, 1941 (2004).
[3] A. S. C. Rittner and J. D. Reppy, Phys. Rev. Lett. **97**, 165301 (2006).
[4] Y. Aoki, J. C. Graves, and H. Kojima, Phys. Rev. Lett. **99**, 015301 (2007).
[5] M. Kondo, S. Takada, Y. Shibayama, and K. Shirahama, J. Low Temp. Phys. **148**, 695 (2007).
[6] A. Penzev, Y. Yasuta, and M. Kubota, J. Low Temp. Phys. **148**, 677 (2007).
[7] S. Balibar and F. Caupin, J. Phys.: Condens. Matter **20**, 173201 (2008).
[8] A. S. C. Rittner and J. D. Reppy, Phys. Rev. Lett. **98**, 175302 (2007).
[9] E. Kim, J. S. Xia, J. T. West, X. Lin, A. C. Clark, and M. H. W. Chan, Phys. Rev. Lett. **100**, 065301 (2008).
[10] A. C. Clark, J. D. Maynard, and M. H. W. Chan, Phys. Rev. B **77**, 184513 (2008).
[11] A. C. Clark, J. T. West, and M. H. W. Chan, Phys. Rev. Lett. **99**, 135302 (2007).
[12] E. Burovski, E. Kozik, A. B. Kuklov, N. V. Prokof'ev, and B. V. Svistunov, Phys. Rev. Lett. **94**, 165301 (2005).
[13] H. Suzuki, J. Phys. Soc. Jpn. **35**, 1472 (1973).
[14] H. Suzuki, J. Phys. Soc. Jpn. **42**, 1865 (1977).
[15] R. Wanner, I. Iwasa, and S. Wales, Solid State Commun. **18**, 853 (1976).
[16] I. Iwasa, K. Araki, and H. Suzuki, J. Phys. Soc. Jpn. **46**, 1119 (1979).
[17] J. R. Beamish and J. P. Franck, Phys. Rev. B **26**, 6104 (1982).
[18] I. Iwasa, N. Saito, and H. Suzuki, J. Phys. Soc. Jpn. **52**, 952 (1983).
[19] J. Day and J. Beamish, Nature (London) **450**, 853 (2007).
[20] A. E. H. Love, *A Treatise on the Mathematical Theory of Elasticity*, 4th ed. (Dover, New York, 1927), p. 287.
[21] J. P. Hirth and J. Lothe, *Theory of Dislocations*, 2nd ed. (Wiley, New York, 1982), p. 26.
[22] I. Iwasa and H. Suzuki, J. Phys. Soc. Jpn. **49**, 1722 (1980).
[23] E. Kim and M. H. W. Chan, Phys. Rev. Lett. **97**, 115302 (2006).
[24] A. Granato and K. Lücke, J. Appl. Phys. **27**, 583 (1956).
[25] M. Boninsegni, A. B. Kuklov, L. Pollet, N. V. Prokof'ev, B. V. Svistunov, and M. Troyer, Phys. Rev. Lett. **99**, 035301 (2007).
[26] J. P. Hirth and J. Lothe, *Theory of Dislocations*, 2nd ed. (Wiley, New York, 1982), p. 361.
[27] L. Pollet, M. Boninsegni, A. B. Kuklov, N. V. Prokof'ev, B. V. Svistunov, and M. Troyer, Phys. Rev. Lett. **101**, 097202 (2008).
[28] A. S. C. Rittner and J. D. Reppy, Phys. Rev. Lett. **101**, 155301 (2008).
[29] Z. Nussinov, A. V. Balatsky, M. J. Graf, and S. A. Trugman, Phys. Rev. B **76**, 014530 (2007).
[30] B. Hunt, E. Pratt, V. Gadagkar, M. Yamashita, A. V. Balatsky, and J. C. Davis, Science **324**, 632 (2009).
[31] C. D. Yoo and A. T. Dorsey, Phys. Rev. B **79**, 100504(R) (2009).
[32] J. T. West, O. Syshchenko, J. Beamish, and M. H. W. Chan, Nat. Phys. **5**, 598 (2009).